

Evolution of Edge states and Critical Phenomena in the Rashba Superconductor with Magnetization

Ai Yamakage,¹ Yukio Tanaka,¹ and Naoto Nagaosa^{2,3}

¹*Department of Applied Physics, Nagoya University, Nagoya, 464-8603, Japan*

²*Department of Applied Physics, University of Tokyo, Tokyo 113-8656, Japan*

³*Cross Correlated Materials Research Group (CMRG), ASI, RIKEN, WAKO 351-0198, Japan*

(Dated: September 30, 2018)

We study Andreev bound states (ABS) and resulting charge transport of Rashba superconductor (RSC) where two-dimensional semiconductor (2DSM) heterostructures is sandwiched by spin-singlet s -wave superconductor and ferromagnet insulator. ABS becomes a chiral Majorana edge mode in topological phase (TP). We clarify that two types of quantum criticality about the topological change of ABS near a quantum critical point (QCP), whether ABS exists at QCP or not. In the former type, ABS has a energy gap and does not cross at zero energy in non-topological phase (NTP). These complex properties can be detected by tunneling conductance between normal metal / RSC junctions.

Topological quantum phenomena and relevant quantum criticality have been an important concept in condensed matter physics [1, 2]. Recently, stimulated by the issue of Majorana fermion in condensed matter physics [3–6], topological quantum behavior of superconductivity becomes a hot topic [7–12]. One of the most crucial point is the property of the non-trivial edge modes in topological phase where edge modes are protected by the bulk energy gap.

The edge state of superconductor has been known from the study of Andreev bound state (ABS) in unconventional superconductors [13–15]. In high T_C cuprate, dispersionless zero energy ABS ubiquitously appears [14, 15] due to the sign change of the pair potential on the Fermi surface. The zero energy state manifests itself as a zero bias conductance peak in tunneling spectroscopy [15, 16]. Subsequently, the presence of ABS with linear dispersion has been clarified in chiral p -wave superconductor [17] realized in Sr_2RuO_4 , where time reversal symmetry is broken [18]. On the other hand, in the presence of spin-orbit(SO) coupling with time reversal symmetry, it has been revealed that spin-singlet s -wave pairing and spin-triplet p -wave one can mix each other due to the broken inversion symmetry [19–21]. ABS appears as a helical edge mode appears for $\Delta_p > \Delta_s$ where we denote s -wave and p -wave pair potentials as Δ_s and Δ_p , respectively, with $\Delta_s > 0$ and $\Delta_p > 0$ [21, 22].

The critical behavior of ABS has been discussed in spin-triplet chiral p -wave pairing [3]. By changing the chemical potential μ of spin-triplet chiral p -wave superconductor from positive to negative, ABS as a chiral Majorana mode disappears. The corresponding quantum critical point is $\mu = 0$. Although, such a quantum phase transition can be possible in $\nu = 5/2$ fractional quantum Hall system [3] and cold atom [23, 24], it is significantly difficult to obtain superconducting state for negative μ in electronic superconductors.

In all of above works, ABS is generated from unconventional pairing with non-zero angular momentum. On the other hand, in the presence of strong SO coupling with broken time reversal symmetry, chiral Majorana modes can be generated from spin-singlet s -wave pairing [25, 26]. Fu and Kane have revealed the presence of chiral Majorana mode at the boundary between ferromagnet and superconductor generated on the

surface of topological insulator (TI). After that manipulating Majorana mode in TI [26] and in semiconductor hetero structures based on conventional spin-singlet s -wave superconductor have been proposed in several contexts [27–29]. Sau *et al.* has proposed a unique Rashba superconductor where two-dimensional electron gas (2DEG) is sandwiched by conventional spin-singlet s -wave superconductor and ferromagnetic insulator [28]. These systems are really promising for future application of quantum qubit since host superconductor is robust against impurity scattering.

Although there have been several theoretical studies about the present RSC [30–32], the feature of the Andreev bound state (ABS) and its relevance to the topological quantum phase transition has not been revealed at all. It is known that ABS emerges as a chiral Majorana edge mode in TP, however, the evolution of ABS in the non-topological phase (NTP) and its connection to quantum phase transition have not been clarified yet. To reveal these problems is indispensable to understand the tunneling spectroscopy of normal metal /RSC junction system and future applications of quantum device.

In this Letter, we study energy dispersions of ABS in RSC composed of 2DEG sandwiched by spin-singlet s -wave superconductor and ferromagnetic insulator. It is clarified that there are two types of quantum criticality for ABS, *i.e.*, quantum phase transition with or without ABS corresponding to type I and type II, respectively. In type I, ABS can exist even at critical point where bulk energy gap closes and in the NTP. Nonzero ABS generated in the NTP does not cross at zero energy. These features are completely different from those in type II where edge states become absent both at the critical point and in the NTP. The conventional criticality of spinless spin-triplet chiral p -wave superconductor belongs to type II [3, 24]. The conductance between normal metal / RSC junction shows wide variety of line shapes reflecting on these novel quantum criticalities. We also show the drastic jump of the conductance at critical point.

A Hamiltonian of Rashba superconductor with magnetization is given by the following form [27–29] :

$$H(\mathbf{k}) = H_0(\mathbf{k}) + H_R(\mathbf{k}) + H_Z + H_S, \quad (1)$$

where kinetic energy H_0 , Rashba spin-orbit interaction

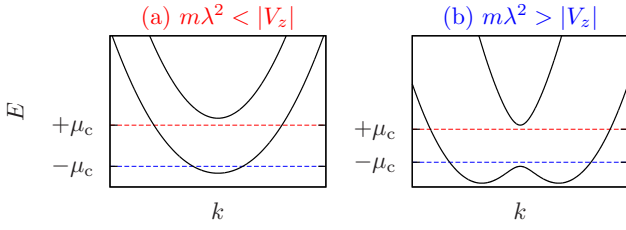


FIG. 1. (color online) Energy spectra of the normal ($\Delta = 0$) states. (a) Zeeman (Rashba spin-orbit) interaction is dominant with $m\lambda^2 < |V_z|$. (b) Rashba spin-orbit interaction is dominant with $m\lambda^2 > |V_z|$. The critical value of chemical potential for the transition between topological and non-topological superconductors is given by $\pm\mu_c = \pm\sqrt{V_z^2 - \Delta^2}$. (see discussion below eq. (6))

(RSOI) H_R , Zeeman interaction H_Z by exchange field from FM insulator, and spin-singlet s -wave pair potential H_S induced by proximity effect are $H_0(\mathbf{k}) = \xi_{\mathbf{k}} s_0 \tau_z$, $H_R(\mathbf{k}) = \lambda(s_x \tau_0 k_y - s_y \tau_z k_x)$, $H_Z = V_z s_z \tau_z$, $H_S = -\Delta s_y \tau_y$, where s and τ are Pauli matrices, s_0 and τ_0 are 2×2 unit matrices, describing electron spin and particle-hole degrees of freedom, respectively. We take the explicit form of kinetic energy as $\xi_{\mathbf{k}} = k^2/2m - \mu$ with μ being chemical potential, for simplicity. The exchange energy in a 2DEG can be tuned by changing the material of ferromagnetic insulator, or tuning the barrier thickness between the ferromagnetic insulator and the 2DEG. In the normal states ($\Delta = 0$), there are two types of the energy bands as shown in Fig. 1. For Zeeman interaction dominant case with $m\lambda^2 < |V_z|$, there are two parabolic dispersions (Fig. 1(a)). On the other hand, for RSOI dominant case with $m\lambda^2 > |V_z|$, the shape of the energy band is wine-bottle like (Fig. 1(b)). As we shall see later, the difference between these two types of energy bands in normal state becomes important.

The eigenvalues of the Hamiltonian for the infinite system are given by $E_a(k_x, k_y) = \sqrt{\eta_k + \zeta_k}$, $E_b(k_x, k_y) = -\sqrt{\eta_k + \zeta_k}$, $E_c(k_x, k_y) = \sqrt{\eta_k - \zeta_k}$, and $E_d(k_x, k_y) = -\sqrt{\eta_k - \zeta_k}$ with

$$\begin{aligned} \eta_k &= \xi_k^2 + \lambda^2 k^2 + V_z^2 + \Delta^2, \\ \zeta_k &= 2\sqrt{(\lambda^2 k^2 + V_z^2)\xi_k^2 + V_z^2 \Delta^2}, \end{aligned} \quad (2)$$

where k is defined by $k = \sqrt{k_x^2 + k_y^2}$ with real k_x and k_y for the plane wave. The corresponding eigenvectors $\mathbf{u}_\alpha(k_x, k_y)$ with $\alpha = a, b, c$, and d are also obtained analytically.

Let us now consider a semi-infinite RSC in $x > 0$ with flat surface at $x = 0$. The wave function in the present system is given by

$$\psi_{k_y, E}(x > 0) = \sum_{i=1}^4 t_i \mathbf{u}_i(q_i, k_y) e^{iq_i x} e^{ik_y y}. \quad (3)$$

When q_i is a real number, the corresponding wave function expresses propagating wave, *i.e.*, scattering state. On the other hand, when q_i is a complex number, it describes an evanescent wave. Energy E and y -component of momentum k_y are good

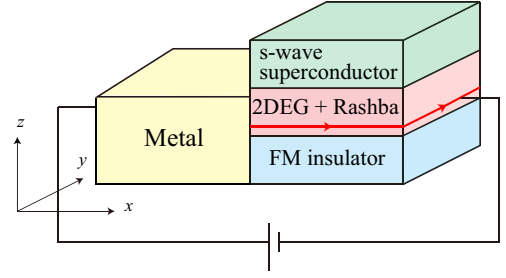


FIG. 2. (color online) Normal metal (N) / Rashba superconductor (RSC) junction. Andreev bound state as edge state can exist denoted by the (red) arrow.

quantum numbers. To obtain q_i , we solve k for fixed $E = E_a(k_x, k_y)$ and $E = E_c(k_x, k_y)$ for $E > 0$ [$E = E_b(k_x, k_y)$ and $E = E_d(k_x, k_y)$ for $E < 0$]. q_i is given by $q_i = k_x$ by postulating the constraints $\partial E_\alpha(q_i, k_y)/\partial q_i > 0$ for scattering state, and $\text{Im}q_i > 0$ for evanescent state. Note here that, in general, k and q_i become complex numbers which can be obtained by analytical continuation. The coefficient t_i is determined by the confinement condition as $\psi_{k_y, E}(0) = 0$.

Tunneling conductance of normal metal (N) / RSC junction as shown in Fig. 2 is calculated based on the standard way [15, 33]. Suppose that the normal metal has no spin-orbit interaction, *i.e.*, the Hamiltonian reads $H_M(\mathbf{k}) = (k^2/2m - \mu_M) s_0 \tau_z$, where $\mu_M = \mu - \epsilon_0$ with ϵ_0 being the energy of bottom of the energy band, which is negative, and the interface potential is given by $H_I = H s_0 \tau_0 \delta(x)$. The wave function in N is given by

$$\begin{aligned} \psi_{k_y, E, s}(x < 0) &= \left[\chi_{se} e^{ik_{ex} x} + \sum_{s' \tau'} r_{ss' \tau'} \chi_{s' \tau'} e^{-i\tau' k_{\tau'} x} \right] e^{ik_y y}, \end{aligned} \quad (4)$$

where the first term denotes an incident electron with spin s , and $\chi_{s\tau}$ is the eigenvector of spin s for electron ($\tau = +1$) or hole ($\tau = -1$), and $k_{ex} = \sqrt{2m(\mu_M + E) - k_y^2}$ and $k_{hx} = \sqrt{2m(\mu_M - E) - k_y^2}$ are momenta of reflected electron and hole, respectively. On the other hand, the wave function in RSC ($x > 0$) obeys the same form as in eq. (3). The boundary condition at the interface located on $x = 0$ is given by the following two expressions [34]. $\psi(-0) = \psi(+0)$, $v(+0)\psi(+0) - v(-0)\psi(-0) = -i2H\tau_z\psi(0)$, where velocity in x -direction is $v(x) = \partial H/\partial k_x|_{k_x \rightarrow -i\partial_x}$. Solving the above equations, we obtain reflection (transmission) coefficient r (t). Charge conductance G normalized by its value G_N in the normal state ($\Delta = 0$) with $V_z = 0$, $\mu/m\lambda^2 = 4$, $\mu_M/m\lambda^2 = 2 \times 10^4$, and $Z^2 = mH^2/\mu_M = 10^4$, which corresponds to the case of Figs. 3(h) and 3(k) with $\Delta = 0$, at

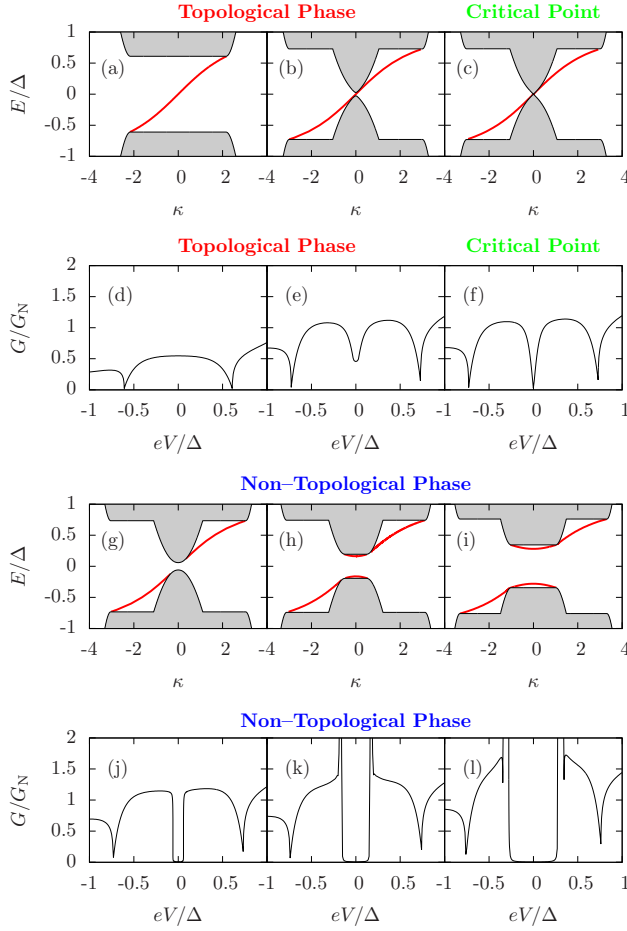


FIG. 3. (color online) Energy spectra and tunneling conductances as a function of bias voltage (eV/Δ) of the Rashba superconductor. The horizontal axis denotes the normalized momentum $\kappa = k_y/\sqrt{m\Delta}$. Zeeman interaction and Rashba spin-orbit interaction are fixed as $V_z/\Delta = 2$, $m\lambda^2/\Delta = 0.5$. The chemical potential is set as follows. (a),(d): $\mu/\Delta = 0$, (b),(e): $\mu/\Delta = 1.7$, (c),(f): $\mu/\Delta = \sqrt{3}$, (g),(j): $\mu/\Delta = 1.8$, (h),(k): $\mu/\Delta = 2$, (i),(l): $\mu/\Delta = 2.5$.

zero bias voltage ($eV = 0$) is given by

$$G/G_N = \frac{\sum_s \int_{-k_F}^{k_F} dk_y T_s(k_y, E)}{\sum_s \int_{-k_F}^{k_F} dk_y T_s(k_y, 0)}, \quad (5)$$

with $T_s(k_y, E) = 2 - \sum_{s'\tau'} \tau' |r_{ss'\tau'}|^2$ and $\mu_M = 2mk_F^2$. Hereafter, the parameters are fixed as $Z^2 = 10$, $\mu_M/\Delta = 10^4$, and all the conductances G are normalized by the same value of G_N .

We discuss the energy spectra and the tunneling conductances, focusing on the difference of the criticality between two RSCs with different chemical potential with $\mu > 0$ (Fig. 3) and $\mu < 0$ (Fig. 4) for $|V_z| > m\lambda^2$.

In TP (Fig. 3(a) and Fig. 4(a)), ABS appears as a chiral Majorana edge mode, where $|V_z| > \sqrt{\mu^2 + \Delta^2}$ is satisfied.

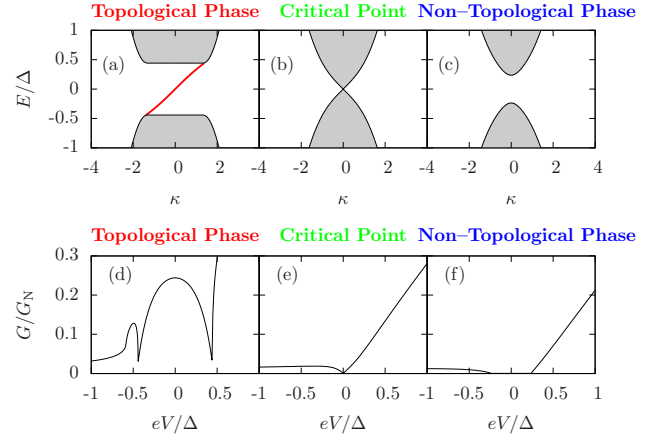


FIG. 4. (color online) Energy spectra (upper) and tunneling conductances (lower) of the Rashba superconductor for negative chemical potentials. (a),(d): $\mu/\Delta = -1$, (b),(e): $\mu/\Delta = -\sqrt{3}$, (c),(f): $\mu/\Delta = -2$. The other parameters are the same as in Fig. 3

Due to the presence of this mode, the corresponding tunneling conductance has a zero bias peak as shown in Fig. 3(d) and Fig. 4(d). For $\mu > 0$, near the QCP [Fig. 3(b)], although ABS appears as a chiral Majorana mode, the corresponding G has a zero bias dip as shown in Fig. 3(e) due to the presence of a parabolic dispersion of bulk energy spectra near $k_y = 0$. At QCP (Fig. 3(c)), it is noted that ABS remains although the bulk energy gap closes at $k_y = 0$. This feature is quite different from $\mu < 0$, where ABS is absent at QCP (Fig. 4(b)). The resulting G has a V -shaped zero energy dip both for two cases shown in Figs. 3(f) and 4(e). For $\mu > 0$, ABS still remains even in the NTP as shown in Figs. 3(g), 3(h), and 3(i). ABS has an energy gap and is absent around $k_y = 0$. The tunneling conductance shows a gap structure around $eV = 0$ [Fig. 3(j)]. With the increase of μ , *i.e.*, away from QCP, the additional non-zero ABS around $k_y = 0$ [Fig. 3(h) and 3(i)] with the almost flat dispersion are generated. As a result, G has two peaks at the corresponding voltages inside the bulk energy gap (Fig. 3(k) and 3(l)). On the other hand, for $\mu < 0$, ABS is absent in NTP as shown in Fig. 4(c). The resulting G is almost zero inside the bulk energy gap (Fig. 4(f)). Based on these results, we can classify two types of criticality whether edge state exists at QCP or not. We denote former type as type I and the latter one as type II in the following.

We have also studied for $|V_z| \leq m\lambda^2$. The energy spectra at QCP with positive μ (Fig. 5(a)) and negative μ (Fig. 5(b)) are shown. In this case, irrespective of the value of μ , ABS exists at QCP. Therefore, the resulting criticality is always type I.

Type I and II transitions can be distinguished experimentally by the line shape of G . In type I transition, line shape of G becomes almost symmetric with respect to $eV = 0$ as shown in Figs. 3(f), 5(c), and 5(d) as compared to that in type II as shown in Fig. 4(f). Furthermore, G at type I transition takes one order of magnitude larger value than that at type II, due to contribution from the edge states.

It is noted that the small value of Z^2 does not qualitatively

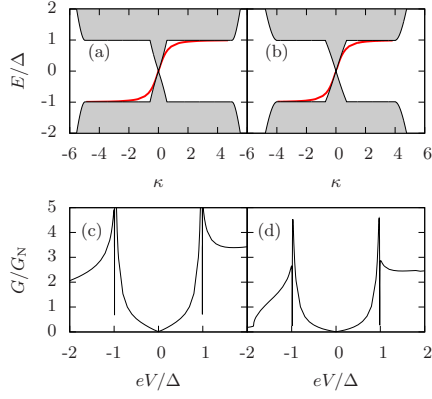


FIG. 5. (color online) Energy spectra and tunneling conductances of the Rashba superconductor for $m\lambda^2 > |V_z|$ at quantum critical point. (a),(c): $\mu/\Delta = \sqrt{1.25}$, (b),(d): $\mu/\Delta = -\sqrt{1.25}$. The other parameters are taken as follows. $m\lambda^2/\Delta = 5$, $V_z/\Delta = 1.5$.

change the results of the paper In the low transparency limit, the contribution from edge states becomes dominant for the conductance G , then the resulting line shape of G becomes insensitive to the parameters of the normal metal, i.e., Z^2 , μ_M , and m . In the present case, the transmission probability in the normal state ($\Delta = 0$) becomes sufficiently small with $G_N/G_0 \sim 10^4$, where G_0 denotes the maximum value of G_N , even for $Z^2 = 0$ since the magnitudes of Fermi momenta in left normal metal ($x < 0$) and right RSC ($x > 0$) are much different with $\mu_M/\mu > 10^3$.

Here, we mention the criticality of ABS in spinless chiral p -wave superconductor. Hamiltonian of spinless chiral p -wave superconductor is given by

$$H_p(\mathbf{k}) = \begin{pmatrix} k^2/2m - \mu & \Delta_p k_- \\ \Delta_p k_+ & -k^2/2m + \mu \end{pmatrix}. \quad (6)$$

It is known that QCP is located at $\mu = 0$. ABS appears as a chiral Majorana mode in TP ($\mu > 0$) while it is absent in NTP $\mu < 0$, respectively [3]. ABS disappears at QCP. In the light of our classification, quantum criticality of spineless chiral p -wave superconductor belongs to the type II.

To understand the difference of two types of criticality, we focus on the energy dispersions in the normal state shown in Fig. 1. Here we introduce the critical value of transition between TP and NTP $\pm\mu_c = \pm\sqrt{V_z^2 - \Delta^2}$. The ABS is generated from $-k_F$ to $+k_F$, where the magnitude of k_F is almost the same with that of the large Fermi surface. First, we focus on the case with $m\lambda^2 < |V_z|$. The type I quantum phase transition occurs at $\mu = \mu_c$, shown in Fig. 3. In this case, the large Fermi surface survives as shown in Fig. 1(a). On the other hand, as shown in Fig. 4, type II quantum phase transition occurs at $\mu = -\mu_c$. In contrast to the type I, the large Fermi surface vanishes in the NTP as shown in Fig. 1(a). For $m\lambda^2 > |V_z|$, the quantum criticality always belongs to type I. Actually, as shown in Fig. 1(b), the large Fermi surface survives both at $\mu = \mu_c$ and $\mu = -\mu_c$. For type I, the number of Fermi surfaces is 2 in NTP and 1 in TP. On the other hand, for

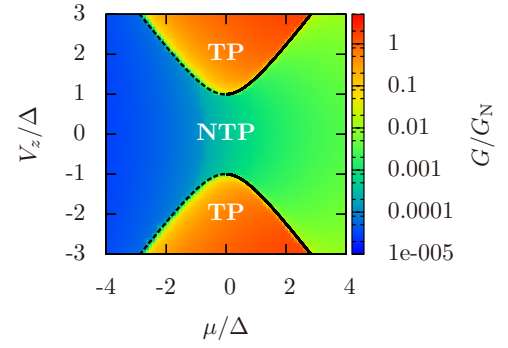


FIG. 6. (color online) Conductance as a function of chemical potential μ/Δ and Zeeman interaction V_z/Δ . Rashba spin-orbit interaction is taken as $m\lambda^2/\Delta = 0.5$. The transition of type I (II) occurs at positive (negative) μ . The solid (broken) line indicates the critical line of type I (II) transition.

type II, the number of Fermi surface is 0 in NTP and 1 in TP. Above rich behavior of quantum criticality in RSC originates from the simultaneous existence of the Rashba spin-orbit coupling and the Zeeman interaction.

Finally, we show the zero-bias tunneling conductance of RSC as a function of μ and V_z in Fig. 6. The quantum phase transition from NTP to TP occurs with tuning the parameter V_z or μ . In accordance with this transition, the conductance increases by about three orders of magnitude, due to the contribution from zero energy ABS at $k_y = 0$.

In this letter, we have calculated the energy spectrum and the tunneling conductance of RSC and clarified its quantum criticality. Quantum phase transition between topological and non-topological superconductors has two types of criticality whether ABS survives or not at QCP. It is remarkable that ABS can remain at QCP in RSC distinctly from spinless chiral p -wave superconductor which is a prototype of topological superconductor. This stems from the structures of Fermi surfaces which are spin-split by Rashba spin-orbit interaction in the normal state. This results can provide a new perspective of quantum criticality for topological superconductors. We have considered only the spin-singlet s -wave superconductor. It is interesting to study in the case of unconventional superconductor where much richer quantum criticality can be expected [35–37].

This work is supported by Grant-in-Aid for Scientific Research (Grants No. 17071007, No. 17071005, No. 19048008, No. 19048015, No. 22103005, No. 22340096, and No. 21244053) from the Ministry of Education, Culture, Sports, Science and Technology of Japan, Strategic International Cooperative Program (Joint Research Type) from Japan Science and Technology Agency, and Funding Program for World-Leading Innovative RD on Science and Technology (FIRST Program).

-
- [1] X. G. Wen: *Quantum Field Theory of Many-Body Systems* (Oxford University Press, Oxford, 2004).
- [2] G. R. Volovik: *The Universe in a Helium Droplet* (Oxford Science Publications, 2003)
- [3] N. Read and D. Green, Phys. Rev. B **61**, 10267 (2000).
- [4] C. Nayak, *et al*, Rev. Mod. Phys. **80**, 1083 (2008).
- [5] S. Das Sarma, C. Nayak, and S. Tewari, Phys. Rev. B **73**, 220502(R) (2006).
- [6] D. A. Ivanov, Phys. Rev. Lett. **86**, 268 (2001).
- [7] A. P. Schnyder, S. Ryu, A. Furusaki, and A. W. W. Ludwig, Phys. Rev. B **78**, 195125 (2008).
- [8] X.L. Qi, T. L. Hughes, S. Raghu and S.C. Zhang, Phys. Rev. Lett. **102**, 187001 (2009).
- [9] R. Roy, arXiv:0803.2868;
- [10] M. Sato, Phys. Rev. B **79**, 214526 (2009); *ibid.* **81**, 220504(R) (2010).
- [11] Y. Tanaka, M. Sato, N. Nagaosa, J. Phys. Soc. Jpn. **81**, 011013 (2011).
- [12] J. Linder, Y. Tanaka, T. Yokoyama, A. Sudbo, N. Nagaosa, Phys. Rev. Lett. **104**, 067001 (2010).
- [13] L. J. Buchholtz and G. Zwicknagl: Phys. Rev. B **23** (1981) 5788; J. Hara and K. Nagai: Prog. Theor. Phys. **76** (1986) 1237.
- [14] C. R. Hu: Phys. Rev. Lett. **72** (1994) 1526.
- [15] S. Kashiwaya and Y. Tanaka, Rep. Prog. Phys. **63**, 1641 (2000).
- [16] Y. Tanaka and S. Kashiwaya, Phys. Rev. Lett. **74**, 3451 (1995).
- [17] M. Matsumoto and M. Sigrist, J. Phys. Soc. Jpn. **68**, 994 (1999); C. Honerkamp and M. Sigrist, J. Low Temp. Phys. **111**, 895 (1998); M. Yamashiro, Y. Tanaka, and S. Kashiwaya, Phys. Rev. B **56**, 7847 (1997); A. Furusaki, M. Matsumoto, and M. Sigrist, Phys. Rev. B **64**, 054514 (2001); M. Stone and R. Roy, Phys. Rev. B **69**, 184511 (2004).
- [18] A. P. Mackenzie and Y. Maeno, Rev. Mod. Phys. **75**, (2003) 657.
- [19] T. Yokoyama, Y. Tanaka and J. Inoue, Phys. Rev. B **72** 220504(R) (2005); C. Iniotakis, N. Hayashi, Y. Sawa, T. Yokoyama, U. May, Y. Tanaka, and M. Sigrist, Phys. Rev. B **76**, 012501 (2007);
- [20] A.B. Vorontsov, I. Vekhter, M. Eschrig, Phys. Rev.Lett. **101**, 127003 (2008).
- [21] Y. Tanaka, T. Yokoyama, A. V. Balatsky and N. Nagaosa, Phys. Rev. B **79**, 060505(R) (2009); M. Sato and S. Fujimoto, Phys. Rev. B **79**, 094504 (2009).
- [22] C. K. Lu and S. Yip, Phys. Rev. B **80**, 024504 (2009).
- [23] S. Tewari, S. Das Sarma, C. Nayak, C. Zhang and P. Zoller, Phys. Rev. Lett., **98**, 010506, (2007).
- [24] T. Mizushima, M. Ichioka and K. Machida, Phys. Rev. Lett., **101**, 150409, (2008).
- [25] L. Fu and C. L. Kane, Phys. Rev. Lett. **100**, 096407 (2008).
- [26] L. Fu and C. L. Kane, Phys. Rev. Lett. **102**, 216403 (2009); A. R. Akhmerov, J. Nilsson, and C. W. J. Beenakker, Phys. Rev. Lett. **102**, 216404 (2009); Y. Tanaka, T. Yokoyama and N. Nagaosa, Phys. Rev. Lett. **103**, 107002 (2009).
- [27] M. Sato, Y. Takahashi, and S. Fujimoto: Phys. Rev. Lett. 103 (2009) 020401; M. Sato, Y. Takahashi, and S. Fujimoto: Phys. Rev. B 82 (2010) 134521.
- [28] J. D. Sau, R. M. Lutchyn, S. Tewari, and S. Das Sarma, Phys. Rev. Lett. **104**, 040502 (2010).
- [29] J. Alicea, Phys. Rev. B **81**, 125318 (2010).
- [30] R. M. Lutchyn, J. D. Sau, and S. Das Sarma, Phys. Rev. Lett. **105** 077001 (2010); Y. Oreg and G. Refael and F. von Oppen, Phys. Rev. Lett. **105**, 177002 (2010); T. Stanescu, R. M. Lutchyn, and S. Das Sarma, Phys. Rev. B **84**, 144522 (2011); J. D. Sau, S. Tewari, R. M. Lutchyn, T. D. Stanescu, and S. Das Sarma, Phys. Rev. B **82**, 214509 (2010); R. M. Lutchyn, T. D. Stanescu and S. Das Sarma, Phys. Rev. Lett. **106** 127001 (2011).
- [31] K. T. Law, P. A. Lee, T. K. Ng, Phys. Rev. Lett. **103**, 237001 (2009); A. C. Potter and P. A. Lee, Phys. Rev. B **83**, 094525 (2011).
- [32] J. Linder and A. Sudbø, Phys. Rev. B 82, 085314 (2010); C. Bena, D. Sticlet and P. Simon, arXiv: 1109.5697; C. Qu, Y. Zhang, L. Mao and C. Zhang, arXiv: 1109.4108; M. Gibertini, F. Taddei, M. Polini and R. Fazio, arXiv:1111.4656.
- [33] G. E. Blonder, M. Tinkham, and T. M. Klapwijk, Phys. Rev. B **25**, 4515 (1982).
- [34] T. Yokoyama, Y. Tanaka, and J. Inoue, Phys. Rev. B **74**, 035318 (2006).
- [35] Y. Tanaka, *et al*, Phys. Rev. Lett. 105 (2010) 097002; K. Yada, M. Sato, Y. Tanaka, and T. Yokoyama: Phys. Rev. B. 83 (2011) 064505.
- [36] M. Sato and S. Fujimoto, Phys. Rev. Lett. **105**, 217001 (2010).
- [37] A. P. Schnyder and S. Ryu, Phys. Rev. B **84**, 060504 (2011); P. M. R. Brydon, A. P. Schnyder, and C. Timm, Phys. Rev. B **84**, 020501 (2011); A. P. Schnyder, P. M. R. Brydon, D. Manske, and C. Timm, Phys. Rev. B **82**, 184508 (2010).